1-1-2012

Reflectance continuum removal spectral index tracking the xanthophyll cycle photoprotective reactions in Norway spruce needles

Daniel Kovac
Global Change Research Centre AS CR, kovac.d@czechglobe.cz

Martin Navratil
University of Ostrava

Zbynek Malenovsky
University of Zürich, zbynek@uow.edu.au

Michal Stroch
Global Change Research Centre AS CR

Vladimir Spunda
Global Change Research Centre AS CR

See next page for additional authors

Reflectance continuum removal spectral index tracking the xanthophyll cycle photoprotective reactions in Norway spruce needles

Abstract

This laboratory experiment tested the ability of the spectral index called 'area under curve normalised to maximal band depth' (ANMB) to track dynamic changes in the xanthophyll cycle of Norway spruce (Picea abies (L.) Karsten) needles. Four-year-old spruce seedlings were gradually acclimated to different photosynthetic photon flux densities (PPFDs) and air temperature regimes. The measurements were conducted at the end of each acclimation period lasting for 11 days. A significant decline in the chlorophylls to carotenoids ratio and the increase of the amount of xanthophyll cycle pigments indicated a higher need for carotenoid-mediated photoprotection in spruce leaves acclimated to high PPFD conditions. Similarly, the photochemical reflectance index (PRI) changed from positive to negative values after changing light conditions from low to high intensity as a consequence of the increase in carotenoid content. Systematic responses of PRI to the de-epoxidation state of xanthophyll cycle pigments (DEPS) were, however, observed only during high temperature treatments and after the exposition of needles to high irradiance. The ANMB index computed from needle reflectance between 507 and 556 nm was able to track dynamic changes in DEPS without any influence induced by changing the content of leaf photosynthetic pigments (chlorophylls, carotenoids).

Keywords

Diurnal course, growth chambers, photosynthetic pigments composition, Picea abies, reflectance continuum removal, xanthophyll cycle

Disciplines

Medicine and Health Sciences | Social and Behavioral Sciences

Publication Details

Kovac, D., Navratil, M., Malenovsky, Z., Stroch, M., Spunda, V. & Urban, O. (2012). Reflectance continuum removal spectral index tracking the xanthophyll cycle photoprotective reactions in Norway spruce needles. Functional Plant Biology: an international journal of plant function, 39 (12), 987-998.

Authors

Daniel Kovac, Martin Navratil, Zbynek Malenovsky, Michal Stroch, Vladimir Spunda, and Otmar Urban

Reflectance continuum removal spectral index tracking the xanthophyll cycle photoprotective reactions in Norway spruce needles

Daniel Kováč[a*], Martin Navrátil[b,c], Zbyněk Malenovský[d,e], Michal Štroch[a,b], Vladimír Špunda[a,b], Otmar Urban[a]

[a]*Global Change Research Centre AS CR, v.v.i., Bělidla 4a, CZ-60300 Brno, Czech Republic*

[b]*Department of Physics, Faculty of Science, University of Ostrava, 30. dubna 22, CZ-70103 Ostrava 1, Czech Republic*

[c]*Karlsruhe Institute of Technology, Botanik II, Kaiserstrasse 12, D-76128 Karlsruhe, Germany*

[d]*Remote Sensing Laboratories, Department of Geography, University of Zürich, Winterthurerstrasse 190, CH-8057 Zürich, Switzerland*

[e]*School of Geography and Environmental Studies, University of Tasmania, Private Bag 76, Hobart 7001, Australia*

**Corresponding author. Email: kovac.d@czechglobe.cz, telephone/fax number: +420 511 192 211*

ABSTRACT

This laboratory experiment tested the ability of the spectral index called Area under curve Normalized to Maximal Band depth (ANMB) to track dynamic changes in the xanthophyll cycle of Norway spruce (*Picea abies*) needles. Four-year old spruce seedlings were gradually acclimated to different photosynthetic photon flux densities (PPFDs) and air temperature regimes. The measurements were carried out at the end of each acclimation period lasting for 11 days. A significant decline in the chlorophylls to carotenoids ratio and the increase of the amount of xanthophyll cycle pigments indicated a higher need for carotenoid-mediated photoprotection in spruce leaves acclimated to high PPFD conditions. Similarly, the Photochemical Reflectance Index (PRI) changed from positive to negative values after changing light conditions from low to high intensity as a consequence of the increase in carotenoid content. Systematic responses of PRI to the de-epoxided state of xanthophyll cycle pigments (DEPS) were, however, observed only during high temperature treatments and after the exposition of needles to high irradiance. The ANMB index computed from needle

reflectance between 507 and 556 nm was able to track dynamic changes in DEPS without any influence induced by changing the content of leaf photosynthetic pigments (chlorophylls, carotenoids).

Key words: *Picea abies*, growth chambers, reflectance continuum removal, xanthophyll cycle, diurnal course, photosynthetic pigments composition

INTRODUCTION

Spatio-temporal estimation of plant photosynthesis at a global scale is required for comprehensive understanding of the terrestrial carbon cycle and the determination of CO_2 uptake by plants (Baldocchi 2003). Carbon flux measurements of eddy-covariance towers have a local character, but can be scaled up to larger areas using specific remote sensing (RS) techniques. A traditional RS approach assessing the vegetation photosynthetic activity via estimation of green plant biomass indicated a close relationship between the Normalized Difference Vegetation Index (NDVI) (Tucker 1979) and the fraction of photosynthetically active radiation (fPAR) absorbed by green vegetation (Myneni and Williams 1994). Spaceborne measurement assessing the amount of fPAR used for photosynthetic processes is, nevertheless, still a challenging task (Grace *et al.* 2007). The Photochemical Reflectance Index (PRI) was applied in several studies to estimate the actual photosynthetic efficiency and other related variables of green vegetation (Garbulsky *et al.* 2011). PRI is a normalized narrowband vegetation index conventionally calculated as $(R_{531} - R_{570})/ (R_{531} + R_{570})$ (Gamon *et al.* 1992), where R is the leaf reflectance at a noted wavelength. Changes in leaf PRI were found to follow dynamic reactions of the xanthophyll cycle that regulates photosynthesis via thermal dissipation of excessive light energy (Demmig-Adams *et al.* 1999).

The width of denotation and the strength of particular physiological signals influencing leaf reflectance are driven by the irradiation, but they are also influenced by differences in leaf anatomy and morphology (Nichol *et al.* 2002). The reflectance change at 531 nm, which is used as a dynamic indicative component in PRI, integrates several processes accompanying the photoprotection reactions. Among them, the xanthophyll cycle pigment interconversion has been identified as a process with a significant impact on the reflectance at around 525 nm. An influence of conformational changes in pigment-binding proteins, which indicates the engagement of xanthophyll cycle pigments to photoprotection, emerges at the wavelengths

above 531 nm (Bilger *et al.* 1989; Gamon *et al.* 1990; Peñuelas *et al.* 1995; Gamon *et al.* 1997).

The link between PRI and the plant physiological status through an understanding of photochemical quenching and non-photochemical quenching processes was investigated by Peñuelas et al. (1995), Dobrowski et al. (2005), Nichol et al. (2006) and Ripullone et al. (2011). The relationship suggested between PRI and photosynthetic efficiency was shown to be inconsistent due to the changes in foliar pigment content and also canopy architecture (Barton and North 2001; Filella *et al.* 2004; Hilker *et al.* 2008b; Suarez *et al.* 2008). The degradation of chlorophylls generally reduces PRI as a result of the increase in reflectance at 570 nm relative to that at 531 nm (Moran *et al.* 2000; Sims and Gamon 2002; Nakaji *et al.* 2006). Hernandez-Clemente (2011) proposed to avoid this issue by using instead a reflectance at around 512 nm as the referential waveband. Finally, Hilker et al. (2010; 2009) demonstrated that PRI can sufficiently indicate the plant physiological status even at the canopy level after correcting differences in viewing angles, which minimized a negative influence of canopy structure on the physiological signal embedded in the reflectance at 531 nm.

Realizing that the photoprotective physiological signal is observable within several wavelengths of a broad blue-green spectral region, the objective of our experiment was to test a new spectrometric indicator of leaf xanthophyll reactions based on the reflectance continuum removal transformation (Broge and Leblanc 2001; Kokaly and Clark 1999). Continuum removal was applied to the spruce needle reflectance within the region of the xanthophyll cycle denotation between 507 – 556 nm. Leaf reflectance was measured in an integrating sphere equipped with a collimated light source. This standard and reproducible measurement set-up ensured stable and accurate reflectance determinations (Gamon and Surfus 1999). Investigated Norway spruce seedlings were exposed to irradiance intensities simulating cloudy and sunny days with moderate and high temperatures to test the robustness of a newly proposed optical indicator towards distinct environmental conditions. During the experimental treatments the plant material was placed into growth chambers to ensure steady environmental conditions. This type of experimental set-up allowed us to evaluate leaf reflectance responses to various physiological states corresponding with particular combinations of air temperature and light intensities. The sensitivity assessment of both optical indices, i.e. PRI and new continuum removal based optical index, to the

photoprotective xanthophyll transformation was supported by the fluorescence measurements of a quantum yield of photosystem II photochemistry (Φ_{PSII}) (Genty *et al.* 1989).

MATERIALS AND METHODS

Plant material and experimental design

Four-year old Norway spruce *(Picea abies (L.) Karsten)* seedlings were gradually acclimated to three regimes differing in environmental conditions inside two growth chambers (HB 1014, Bioline-Heraeus, Hanau, Germany). The duration of each acclimation regime was 11 days. The daily courses of particular microclimatic parameters for the individual acclimation regimes are shown in Fig. 1.

The seedlings of both chambers were initially acclimated to a low photosynthetic photon flux density (PPFD) irradiance and moderate air temperature (T_{air}) (LI-LT acclimation regime) with maximum PPFD at 'midday' of 300 μmol m^{-2} s^{-1} and T_{air} in the range of 15–25°C. In both chambers PPFD was then increased to reach a 'midday' maximum of 1000 μmol m^{-2} s^{-1} (HI regime). In one chamber, the daily course of T_{air} remained unchanged (HI-LT regime), whereas in the second growth chamber the daily course of T_{air} ranged from 20–35°C, resulting in a high irradiance and high air temperature (HI-HT) acclimation regime. For the last acclimation regime the irradiation conditions of both chambers remained high (HI), whereas the temperature was increased. In the first growth chamber, low T_{air} (LT) was increased to high T_{air} (i.e. resulting in HI-HT regime), whereas T_{air} in the second growth chamber was increased even further to 25-40°C (HI-HT2 regime). The plants of both growth chambers were sufficiently watered (200 ml per plant/day). Relative air humidity was kept between 50 and 65% in all treatments. Daily increases in PPFDs for LI regimes were set to 10, 100, 160 and 300 μmol m^{-2} s^{-1}, and to 25, 300, 500 and 1000 μmol m^{-2} s^{-1} for HI regimes (Fig. 1). Due to the horizontal heterogeneity of the illumination inside the growth chambers, the incident PPFDs for the measured shoots varied up to 10%, when compared to the computed average PPFDs.

All experiments were carried out on current and one-year old needles collected from the two uppermost whorls of the seedlings, where the incident irradiance was ensured to reach the predefined PPFD levels (see Fig. 1). Prior to each measurement cycle, the spruce seedlings were acclimated to the actual environmental conditions for at least half an hour. The

132 measurements were conducted at predawn (before the light in the chambers was turned on at
133 8:30 and 10:00 am), in the morning (around 10:30 - 13:30), at noon (around 14:00 - 17:00),
134 and in the afternoon (around 17:30 - 20:30) of simulated daily courses. Each measuring cycle
135 consisted of needle reflectance determination, needle collection for analysis of photosynthetic
136 pigment content and the fluorescence measurement. The needle samples were collected from
137 five trees of each growth chamber, and two reflectance measurements were carried out per
138 sample. The samples were kept in growth chamber conditions during the whole measurement.
139 To avoid misrepresentation of DEPS acquisitions due to the reflectance measurement, needles
140 lined up in the carrier were kept inside the growth chamber for 10 minutes at the required
141 irradiance for pre-adaptation. Their reflectance was measured from the illuminated side. The
142 very same needles were used for the xanthophyll analysis performed with an HPLC system
143 and spectrometric assessment of chlorophylls and carotenoids. After scanning the needle
144 sample for gap fraction estimation, it was illuminated once again for additional 5 minutes.
145 The light-adapted needles were stored in liquid nitrogen. The full measurement procedure,
146 starting from needle detachment until freezing needle samples in liquid nitrogen, took a total
147 of about 20 minutes. Since our previous laboratory tests showed no significant change in
148 DEPS of spruce needles within the first 30 minutes after the shoot detachment (Štroch,
149 unpublished data), this should be an acceptable processing time without a significant
150 influence on the leaf xanthophyll composition. Finally, the chlorophyll *a* fluorescence
151 parameters were measured at the same spot of each marked tree throughout the whole
152 experiment.
153
154 *Reflectance measurements*
155
156 The leaf reflectance of the spruce needles sampled was measured according to the method of
157 Daughtry et al. (1989) modified by Malenovský et al. (2006a). The LI-1800 spectroradiometer
158 (Li-Cor Inc., Lincoln, NE, USA) coupled with an integrating sphere LI-1800-12 (Li-Cor,
159 USA) was used to acquire the spruce needle reflectance measurements between 400 and 1100
160 nm, with a wavelength interval of 1 nm. The directional-hemispherical reflectance of the
161 sampled needles was computed based on the following equation:
162 $$R = \frac{R_{TOTAL} / R_{REF}}{1 - GF}\ , \qquad \text{(Eq. 1)}$$

where R_{TOTAL} is the flux of radiation reflected from the sample in reflectance mode, R_{REF} is the flux of radiation reflected from a $BaSO_4$ reference standard in reference mode and GF is the gap fraction between the sample needles illuminated in the reflectance mode. Needles tied up in a sample holder were scanned using a double lamp digital scanner to compute the sample (GF) (Mesarch *et al.* 1999). GF was obtained via image processing, determined as the number of pixels of the total gap area between the illuminated needles divided by the number of pixels of the total (illuminated) area measured.

Concept of the $ANMB_{507\text{-}556}$ index

Continuum removal is a mathematical, reflectance normalizing transformation (Clark and Roush 1984; Kokaly and Clark 1999; Broge and Leblanc 2001) that allows the comparison of individual absorption features based on their common baseline. Continuum removal enhances reflectance bands by correcting apparent shifts in the band maximum caused by wavelength dependent scattering. The concept of a newly tested continuum removal based optical index called Area under curve Normalized to Maximum Band Depth (ANMB) has been described in detail in the peer-reviewed article by Malenovský et al. (2006b). The continuum removal transformation was applied to the measured needle directional-hemispherical reflectance between 507 and 556 nm to isolate the reflectance signal affected by the xanthophyll cycle. A spectral interval between 507 and 556 nm was selected to include two known spectral features related to the interconversion of xanthophyll cycle pigments: i) a subtle absorbance between 505 and 515 nm (Bilger *et al.* 1989) and ii) a broader reflectance change at around 531 nm with two contributing components located at 526 and 545 nm (Gamon *et al.* 1997). The wavelength extent of the xanthophyll-induced reflectance change is difficult to assess due to a specific boundary of particular pigments on the binding proteins, and dynamic changes in the chemical environment within the leaves (Ustin *et al.* 2006).

In our experiment, the continuum removal transformation was applied to the needle reflectance according to Kokaly and Clark (1999). The reflectance at a particular wavelength was normalized to the value of the same wavelength, which is located on a straight line interpolated linearly between the reflectance values at 505 and 556 nm. Then, the Area Under Curve ($AUC_{507\text{-}556}$) was computed as the integration of the area under the continuum-removed reflectance according to the equation:

$$AUC_{507-556} = \frac{1}{2}\sum_{i=1}^{n-1}(\lambda_{i+1} - \lambda_i)(R_{CR(\lambda i+1)} + R_{CR(\lambda i)}), \quad \text{(Eq. 2)}$$

where $R_{CR(\lambda i)}$ and $R_{CR(\lambda i+1)}$ are the continuum-removed reflectance values of the spectral bands λ_i and λ_{i+1} in the wavelengths i and $i+1$ located within the selected spectral interval, and n is the number of spectral bands, which is equal to 50 for the given spectral interval of 507 – 556 nm and the resolution of 1 nm. Finally, $ANMB_{507-556}$ was computed as the ratio of $AUC_{507-556}$ and a maximal band depth of the continuum-removed reflectance between 507-556 nm ($MBD_{507-556}$):

$$ANMB_{507-556} = \frac{AUC_{507-556}}{MBD_{507-556}}. \quad \text{(Eq. 3)}$$

The purpose of normalization by $MBD_{507-556}$ was to emphasize changes in the reflectance continuum-removed spectral bands adjacent to that in which $MBD_{507-556}$ is located.

Analysis of photosynthetic pigments

The contents of foliar pigments, i.e. the total chlorophylls (Chl *a*+*b*) and total carotenoids (Car *x*+*c*), and also the Chl *a*/*b* and Chl *a*+*b*/Car *x*+*c* ratios were measured with the spectrophotometer UV/VIS 550 (Unicam, Cambridge, England) from supernatant obtained after the centrifugation (for 3 min at 480 g) of pigment extracts in 80% acetone with a small amount of $MgCO_3$. The contents of needle pigments were determined according to equations by Lichtenthaler (1987). Chl *a*+*b* and Car *x*+*c* contents were expressed per needle projection area that was estimated from digital images of the needles analyzed. The needle images were recorded with a standard table scanner and their projections were estimated using the Cernota software (Kalina and Slovák 2004).

The content of xanthophyll cycle pigments, i.e. antheraxanthin (A), violaxanthin (V), and zeaxanthin (Z), was estimated by the gradient reversed-phase HPLC (TSP Analytical, Kent City, USA) (Kurasová *et al.* 2003). The conversion factors for contents of the individual carotenoids were used according to Färber and Jahns (1998). The conversion state of the xanthophyll cycle pigments (de-epoxidation state; DEPS) was calculated as:

DEPS = (A + Z)/ (V + A + Z) (Gilmore and Björkman 1994). (Eq. 4)

Measurements of quantum yield of photosystem II photochemistry

The quantum yield of photosystem II photochemistry (Φ_{PSII}) was measured directly on shoots of the trees under the actual PPFD and T_{air} conditions using a portable chlorophyll fluorometer (PAM-2000, Heinz Walz, Effeltrich, Germany). The measurements were carried out after at least 30 min of exposure to the given growth conditions in the morning, at noon and in the afternoon (i.e. under PPFDs of 100 and 300 μmol m^{-2} s^{-1} for LI plants and 300 and 1000 μmol m^{-2} s^{-1} for HI plants). The corresponding $\Phi_{PSII,}$ was calculated according to Genty et al. (1989):

$$\Phi_{PSII} = (F_M' - F_S)/F_M', \quad \text{(Eq. 5)}$$

where F_S is the steady-state fluorescence and F_M' is the maximum fluorescence emission obtained after the application of the saturating light pulse lasting for 0.8 s and producing incident PPFD > 3500 μmol m^{-2} s^{-1}.

Data analysis

Statistical differences between the means of leaf pigment characteristics were tested using a two-sample F-test for variances, followed by a Student's t-test computed at level of significance $P < 0.05$. The Student's t-test was applied based on the results of the F-test, assuming either equal or unequal variances. A nonparametric Mann–Whitney U-test was used to compare datasets with uneven numbers of elements. The determination coefficient (R^2) was computed to express the variation percentage of a dependent variable explained by an established regression with the independent variable. The significance of the statistical model was tested at probability levels $P < 0.05$, $P < 0.01$ and $P < 0.001$, using the analysis of variance (ANOVA). All data analyses and statistical tests were carried out with the mathematical-statistical software R (R Development Core Team 2010).

RESULTS AND DISCUSSION

Changes in photosynthetic pigments composition during acclimation regimes

Throughout all the experiments a needle morphological parameter called specific leaf area (SLA), which is defined as the ratio of leaf area to dry weight, was invariant (Fig. 2A). We, therefore, assume that all the needles in our experiment had comparable geometrical proportions (in particular needle thickness). Contrary to SLA, the content of photosynthetic

pigments varied between the acclimation regimes. Increases in incoming irradiation during LT treatment favored the synthesis of chlorophylls, whereas the transition of plants to HT conditions promoted the degradation of foliar chlorophylls (Fig. 2B). Although the Chl *a*+*b* increase in the case of acclimation to HI-LT and also the Chl *a*+*b* decrease in the case of acclimation to HI-HT are insignificant, the Chl *a*+*b* difference between LT and HT treatments is significant at $P < 0.05$ (Student's t-test). A temperature increase also led to a chlorophyll degradation in the HI-LT acclimated plants. Chl *a*+*b* for the HI-HT2 acclimation regime seems to be slightly higher when compared to the HI-HT plants at the end of the acclimation. However, this difference is not statistically significant.

A clear overview of the foliar pigment composition is offered by the pigment ratios in Fig. 3. The response of the pigment composition in spruce needles upon acclimation to the HI regime corresponds with the typical reactions of plants exposed to enhanced irradiances. As the light-harvesting complexes possess quite a low Chl *a/b* ratio, this ratio can be used as an indirect indicator of the size of photosystem II (PSII) light-harvesting complexes (LHCII) (van Amerongen and van Grondelle 2001). Chl *a/b* is higher in spruce needles acclimated to the HI regime than to the LI regime irrespective of the temperature (Fig. 3A). Still, the difference in Chl *a*/*b* of needles acclimated to LI and HI conditions was found to be statistically insignificant. Just a slight increase in the Chl *a/b* ratio may indicate a negligible LHCII reduction, but one has to keep in mind that the Chl *a/b* ratio is also influenced by the change in the PSII/photosystem I (PSI) stoichiometry. According to Thayer and Björkman (1992) Chl *a/b* is higher in PSI than in PSII. An increase of the PSII/PSI ratio typically observed in the case of high intensity light acclimation tends to decrease Chl *a/b*, acting against the effect of the LHCII reduction. (když se nad tím krutopřísně pozastavím, chceme ukázat nebo se zastavujeme nad tím proč jsou pigmenty jaké jsou, konktrétní hypotézu netestujeme – myslím podání rozložení pigmentů v rostlině; extra bota to snad není) -> Toto si musis rozhodnout sam nebo s Otikem, ja nejsem odbornik na LHCII ani PSII/PSI, etc.

A more reliable indicator of the LHCII apportionment is, therefore, the Chl *a*+*b*/Car *x*+*c* ratio. In comparison to the reaction centers, the LHCII proteins show a high Chl *a*+*b*/Car *x*+*c* ratio (Sarijeva *et al.* 2007). Consequently, a significant decrease in the Chl *a*+*b*/Car *x*+*c* ratio (Fig. 3B) indicates a rapid LHCII reduction upon acclimation to the HI regime, which is not observable within the Chl *a/b* ratio changes. On one hand, decreases of Chl *a*+*b*/Car *x*+*c* in the HI-LT and HI-HT2 treatments are associated with an increase in the Car *x*+*c* content per unit needle area (Fig. 2C). This observation indicates the synthesis of PSII reaction centers,

which, as discussed previously, complicates the usage of Chl *a/b* as the indicator of LHCII size. On the other hand, a decrease of Chl *a*+*b*/Car *x*+*c* in the case of the HI-HT treatment in chamber two is result of Chl *a*+*b* decline (Fig. 2C). Chl *a/b* of these plants remained unchanged (Fig. 3A).

The observed decrease of the Chl *a*+*b*/Car *x*+*c* ratio after an 11-day exposure to HI indicates an enhanced need for carotenoid-mediated photoprotection under the HI regime (Behera *et al.* 2002). A dissipation of excess light energy in Norway spruce needles is efficiently mediated by transformation of the xanthophyll cycle pigments (Štroch *et al.* 2008) that can be non-destructively observed using PRI (Peñuelas *et al.* 1995). The amount of xanthophyll cycle pigments rose significantly upon acclimation to the HI regime (Fig. 3C), demonstrating an increasing demand for thermal dissipation of excessive light energy occurring under HI conditions. The observed increase of the VAZ content accompanied by the reduction of LHCII after HI acclimation is in agreement with previously published results by Demmig-Adams and Adams (1996), Kurasová *et al.* (2002) or Lichtenthaler *et al.* (2007).

After the acclimation to LI-LT conditions, spruce needles started the light period with DEPS between 30-40 % (Fig. 4), while at the end of the HI acclimation, predawn DEPS raised significantly to 40-55 % ($P < 0.05$, Student's t-test). As expected, the maximal DEPS was always observed during the midday period under the most severe illumination intensity (DEPS of 85-90 % during the HI regime), when plants had the highest demand of the xanthophyll-mediated photoprotection. Such high DEPS values are in accordance with results by Kurasová *et al.* (2003) showing very efficient V de-epoxidation in the photosynthetic apparatus of Norway spruces when compared to other plant species.

Dynamic temporal changes in PRI and $ANMB_{507-556}$

Daily courses of PRI measured during all treatments are shown in Fig. 5. Based on findings of Peñuelas et al. (1995), a rapid reduction in PRI can be expected after the exposition of evergreen plants to excessive irradiation. Comparison of the results in Fig. 5 and Fig. 4, suggests, however, a rather low correlation of PRI with xanthophyll cycle pigment changes induced by irradiation changes. PRI remained almost invariant under the low light intensities in both growth chambers. One can observe midday PRI decline only under the HI-HT and HI-HT2 regimes and also a systematic shift from positive to negative values after the acclimation to high irradiation treatments (Fig. 5). These are the only two significant changes observed in

PRI values measured ($P < 0.05$, Mann–Whitney U-test). According to Garrity et al. (2011), PRI responds not only to the actual content of carotenoids, driving particularly the spectral response at 531 nm, but to some extent it is also influenced by chlorophyll absorption at 570 nm. Since needle Chl *a*+*b* increased after acclimation to the HI-LT regime in the first growth chamber, but decreased after acclimation to the HI-HT regime in the second chamber (Fig. 2B), this shift cannot be attributed solely to the varying Chl *a*+*b* content as published previously by Moran el al. (2000) or by Sims and Gamon (2002). The observed negative PRI most likely results from a decrease in Chl *a*+*b*/ Car *x*+*c* ratio (compare Fig. 3BC and Fig. 5), as reported by Stylinsky et al. (2002) and also by Guo et al. (2006) for various plant species. Nevertheless, it is important to note that the PRI of plants acclimated to HI-HT2 conditions, after Chl *a*+*b*/ Car *x*+*c* reaching minimum value, remained comparable with the PRI of other HI treatments.

Fig. 6 shows the daily courses and the statistically significant changes in $ANMB_{507\text{-}556}$ ($P < 0.05$, Mann–Whitney U-test) for all the irradiation-temperature regimes tested. During the simulated daytime periods, the dynamics of mean $ANMB_{507\text{-}556}$ closely followed changes in light intensity, irrespective of the air temperature inside the growth chambers. $ANMB_{507\text{-}556}$ decreased from morning until midday and subsequently increased in the afternoon as a consequence of changing photon absorption within the examined spectral region. Fig. 7 demonstrates changes observed in the shape of the reflectance signal between 507 and 556 nm in relation to the leaf xanthophyll de-epoxidation. To illustrate the change, the $MBD_{507\text{-}556}$ normalized continuum-removed reflectance (Fig. 7B) of two needle samples (the first one with DEPS ~ 50% and the second one with DEPS ~ 85%) was subtracted from the same needle reflectance transformation of a sample with DEPS ~ 30% (serving as a baseline). Fig. 7C shows a large negative difference in the $MBD_{507\text{-}556}$ normalized continuum-removed reflectance with a local maximum at around 526 nm and a smaller but steady positive difference between 535 and 550 nm, both of them getting larger with an increasing xanthophyll DEPS. This result is in line with the finding by Gamon et al. (1997) that the 526-nm component correlates more strongly with the xanthophyll pigment conversion compared to the 545-nm component. However, Gamon et al. (1997) also noted that both components are functionally interconnected and should not be treated separately, as the 526-nm component occurs only in the presence of the 545-nm component. Although these findings favor our choice of the 507 – 556 nm reflectance as a suitable interval for ANMB computation it is important to mention that also other similar wavelength intervals, including the spectral

changes induced by the violaxanthin deepoxidation, can potentially provide comparable results.

A closer investigation of the measured needle spectral signatures revealed that a GF between the needles presented at the sample port of the integrating sphere does, to a certain extent, influence the reflectance amplitude, and also the values of the parameter $ANMB_{507-556}$. Studies focused on measuring optical properties of conifer leaves advise to keep the GF between 0.3 and 0.5 (e.g. Mesarch et al., 1999). Unfortunately, due to the limited amount of available plant material (only six spruce seedlings could be placed in one growth chamber), the GF size of needle samples measured in our experiment was slightly higher, ranging from 0.45 to 0.6. A statistically significant linear regression was found between the GF size and $ANMB_{507-556}$ for the group of samples with DEPS between 40 and 55% ($R^2 = 0.53$, $P < 0.001$, $n = 42$; data not shown). Although this outcome suggests a negative dependency of $ANMB_{507-556}$ on GF, this dependency is non-systematically distributed across the measurements of all irradiation-temperature treatments. Computing a mean of the repetitive spectral measurements and the use of the boxplot representation minimize the impact of the non-systematic GF influence in our leaf reflectance measurements. Considering this fact, we are confident that the temporal responses of mean $ANMB_{507-556}$ (Fig. 6) do not reflect changes in GF but follow daily changes in DEPS of the xanthophyll cycle pigments (Fig. 4). (krutopřísný recenzent namítne že udaj R2 neříká nic o směrnici) -> smernice je zminena: a negative dependency of ANMB507-556 on GF.

Statistical relationships of vegetation indexes with DEPS and Φ_{PSII}

A statistically significant linear regression established between PRI and DEPS ($R^2 = 0.34$, $P < 0.01$, Fig. 8A) implies that PRI is able to explain about 34% of the DEPS variability. Compared to this result, a stronger mutual correlation was revealed between $ANMB_{507-556}$ and DEPS. The linear regression testing the statistical dependency of $ANMB_{507-556}$ on corresponding DEPS values resulted in $R^2 = 0.64$ ($P < 0.001$, Fig. 8B) in the case of 24 mean index values, and $R^2 = 0.53$ ($P < 0.001$) when tested for single spectral measurements (data not shown). The $ANMB_{507-556}$-DEPS statistical dependency is weakened mainly by the afternoon measurements of the second day, when DEPS was persistently high in both chambers (Fig. 4), whereas $ANMB_{507-556}$ already started to relax (Fig. 6). In spite of this, $ANMB_{507-556}$ exhibits the ability to follow DEPS independently of the size of the VAZ pool

and Chl $a+b$/Car $x+c$ ratio, which both varied significantly among needles acclimated to different microclimatic conditions (Fig. 3). Also, a varying needle chlorophyll content (Fig. 2B) does not seem to affect the ability of $ANMB_{507-556}$ to capture the dynamics of the xanthophyll cycle pigments. The regression between $ANMB_{507-556}$ and DEPS is strong across samples that vary considerably in content of these photosynthetic pigments.

Investigation of the changes in the quantum yield of photosystem II photochemistry (Φ_{PSII}) (Fig. 9) revealed similar relationships for both spectral indices (Fig. 10). Statistically significant linear regressions with $R^2 = 0.57$ and $R^2 = 0.48$ ($P < 0.001$) were established for PRI and $ANMB_{507-556}$, respectively. These results suggest a lower sensibility of both optical indices to Φ_{PSII}, especially for low Φ_{PSII} values (Fig. 10). In the case of PRI, the index remained low at the end of the acclimation to the HI-HT2 regime, which corresponds with Φ_{PSII} of about 60%. The same Φ_{PSII} was observed at noon for HI-LT acclimated plants, but without a noticeable decrease in PRI (compare Fig. 9 and Fig. 5). Busch *et al.* (2009) also reported a weak relationship between PRI and Φ_{PSII} measured for Jack pine *(Pinus Banksiana)* seedlings. They observed Φ_{PSII} being related mainly to the changes in temperature, whereas PRI followed changes in light intensity. In our experiment, PRI seems to respond rather to increased temperature stress, which may demonstrate a low capacity of evergreen conifers from the cold regions to adjust their temperature optimum for photosynthesis (Way and Sage 2008).

Although the $ANMB_{507-556}$ dynamic can follow temporal changes in DEPS, its dependency on Φ_{PSII} is weaker and less consistent (Fig. 10B). This result points out the necessity to examine responses of $ANMB_{507-556}$ to more complex changes in the photosynthesis performance. A high water vapour pressure deficit induces stomata closure which, consequently, reduces the CO_2 diffusion into the leaf interior and limits plant photosynthetic processes (e.g. Štroch *et al.* 2010). Since the relative air humidity of our experiments was kept stable (between 50 – 65 %), the behavior of $ANMB_{507-556}$ under natural conditions, where the relative air humidity can drop even lower and the incidence of solar irradiation can reach intensities higher than 1000 $\mu mol\ m^{-2}\ s^{-1}$, still has to be investigated. Therefore, future studies should be focused on plants that manage and regulate even more excessive irradiation. Secondly, the ability of $ANMB_{507-556}$ to track dynamic transformations of the xanthophyll cycle pigments needs to be tested for plant species of both photosynthetic pathways (C3 and C4 plants), growing in their natural environment. Since several recent studies demonstrated a negative influence of the complex canopy structure (e.g. a conifer forest) on the performance of PRI (Hilker *et al.* 2008a; Suarez

et al. 2008; Hernandez-Clemente *et al.* 2011), the sensitivity of the $ANMB_{507-556}$ index to canopy architecture needs to be investigated before its application to airborne and spaceborne remote sensing data.

CONCLUSION

This study demonstrates the potential of the $ANMB_{507-556}$ reflectance continuum removal index to indicate the actual status of the xanthophyll-based photochemical protective processes in plants. Norway spruce needles react to increasing light intensity and temperature by rapid changes in their photosynthetic pigment composition. This acclimation is accompanied by large adjustments in the content of chlorophylls and carotenoids and, in particular, of xanthophylls. $ANMB_{507-556}$ was able to follow the dynamic changes in the de-epoxidation state of the xanthophyll pigments, while neither being affected by temperature increase nor by content alterations in needle chlorophylls and carotenoids. PRI demonstrated a similar dynamic behavior as $ANMB_{507-556}$, but only under the combined irradiation-temperature stress conditions. Although our statistical test revealed a significant relationship of photoprotective xanthophyll reactions and $ANMB_{507-556}$ computed from the leaf reflectance of Norway spruce needles, it still needs to be verified by follow-up laboratory or field experiments carried out with other plant species. If approved, it might become a perspective spectral indicator for remote sensing, especially for airborne/spaceborne imaging spectroscopy observations of the vegetation canopy light use efficiency.

ACKNOWLEDGEMENT

This work is part of the research supported by the grant ForChange (SP/2D1/70/08, Ministry of Environment of the Czech Republic), CzeCOS/ICOS (LM2010007, Ministry of Education CR), and by the OP RDI projects CzechGlobe (CZ.1.05/1.1.00/02.0073) and the Institute of Environmental Technologies (CZ.1.05/2.1.00/03.0100). We thank Mrs. Běla Piskořová and Hana Válková for technical assistance and Mrs. Gabrielle Johnson for English language editing.

REFERENCES

455 Baldocchi DD (2003) Assessing the eddy covariance technique for evaluating carbon dioxide
456 exchange rates of ecosystems: past, present and future. *Global Change Biology* **9**, 479-492.
457
458 Barton CVM, North PRJ (2001) Remote sensing of canopy light use efficiency using the
459 photochemical reflectance index - Model and sensitivity analysis. *Remote Sensing of*
460 *Environment* **78**, 264-273.
461
462 Behera RK, Mishra PC, Choudhury NK (2002) High irradiance and water stress induce
463 alterations in pigment composition and chloroplast activities of primary wheat leaves. *Journal*
464 *of Plant Physiology* **159**, 967-973.
465
466 Bilger W, Björkman O, Thayer SS (1989) Light-induced spectral absorbance changes in
467 relation to photosynthesis and the epoxidation state of xanthophyll cycle components in
468 cotton leaves. *Plant Physiology* **91**, 542-551.
469
470 Broge NH, Leblanc E (2001) Comparing prediction power and stability of broadband and
471 hyperspectral vegetation indices for estimation of green leaf area index and canopy
472 chlorophyll density. *Remote Sensing of Environment* **76**, 156-172.
473
474 Busch F, Huner NPA, Ensminger I (2009) Biochemical constrains limit the potential of the
475 photochemical reflectance index as a predictor of effective quantum efficiency of
476 photosynthesis during the winter spring transition in Jack pine seedlings. *Functional Plant*
477 *Biology* **36**, 1016-1026.
478
479 Clark RN, Roush TL (1984) Reflectance spectroscopy - quantitative analysis techniques for
480 remote-sensing applications. *Journal of Geophysical Research* **89**, 6329-6340.
481
482 Daughtry CST, Ranson KJ, Biehl LL (1989) A new technique to measure the spectral
483 properties of conifer needles. *Remote Sensing of Environment* **27**, 81-91.
484
485 Demmig-Adams B, Adams WW (1996) Xanthophyll cycle and light stress in nature: Uniform
486 response to excess direct sunlight among higher plant species. *Planta* **198**, 460-470.
487

488 Demmig-Adams B, Adams WW, Ebbert V, Logan BA (1999) Ecophysiology of the
489 xanthophyll cycle. In 'Photochemistry of Carotenoids' pp. 245-269. (Kluwer Academic Publ:
490 Dordrecht)
491
492 Dobrowski SZ, Pushnik JC, Zarco-Tejada PJ, Ustin SL (2005) Simple reflectance indices
493 track heat and water stress-induced changes in steady-state chlorophyll fluorescence at the
494 canopy scale. *Remote Sensing of Environment* **97**, 403-414.
495
496 Färber A, Jahns P (1998) The xanthophyll cycle of higher plants: influence of antenna size
497 and membrane organization. *Biochimica Et Biophysica Acta-Bioenergetics* **1363**, 47-58.
498
499 Filella I, Peñuelas J, Llorens L, Estiarte M (2004) Reflectance assessment of seasonal and
500 annual changes in biomass and CO2 uptake of a Mediterranean shrubland submitted to
501 experimental warming and drought. *Remote Sensing of Environment* **90**, 308-318.
502
503 Gamon JA, Field CB, Bilger W, Björkman O, Fredeen AL, Peñuelas J (1990) Remote sensing
504 of the xanthophyll cycle and chlorophyll fluorescence in sunflower leaves and canopies.
505 *Oecologia* **85**, 1-7.
506
507 Gamon JA, Peñuelas J, Field CB (1992) A NarrowWaveband Spectral Index That Tracks
508 Diurnal Changes in Photosynthetic Efficiency. *Remote Sensing of Environment* **41**, 35-44.
509
510 Gamon JA, Serrano L, Surfus JS (1997) The photochemical reflectance index: an optical
511 indicator of photosynthetic radiation use efficiency across species, functional types, and
512 nutrient levels. *Oecologia* **112**, 492-501.
513
514 Gamon JA, Surfus JS (1999) Assessing leaf pigment content and activity with a reflectometer.
515 *New Phytologist* **143**, 105-117.
516
517 Garbulsky MF, Peñuelas J, Gamon J, Inoue Y, Filella I (2011) The photochemical reflectance
518 index (PRI) and the remote sensing of leaf, canopy and ecosystem radiation use efficiencies A
519 review and meta-analysis. *Remote Sensing of Environment* **115**, 281-297.
520

521 Garrity SR, Eitel JUH, Vierling LA (2011) Disentangling the relationships between plant
522 pigments and the photochemical reflectance index reveals a new approach for remote
523 estimation of carotenoid content. *Remote Sensing of Environment* **115**, 628-635.
524
525 Genty B, Briantais JM, Baker NR (1989) The relationship between the quantum yield of
526 photosynthetic electron transport and quenching of chlorophyll fluorescence *Biochimica Et*
527 *Biophysica Acta* **990**, 87-92.
528
529 Gilmore AM, Björkman O (1994) Adenine nucleotides and the xanthophyll cycle in leaves. II.
530 Comparison of the effects of CO2- and temperature-limited photosynthesis on photosystem II
531 fluorescence quenching, the adenylate energy charge and violaxanthin de- epoxidation in
532 cotton. *Planta* **192**, 537-544.
533
534 Grace J, Nichol C, Disney M, Lewis P, Quaife T, Bowyer P (2007) Can we measure terrestrial
535 photosynthesis from space directly, using spectral reflectance and fluorescence? *Global*
536 *Change Biology* **13**, 1484-1497.
537
538 Guo JM, Trotter CM, Newton PCD (2006) Initial observations of increased requirements for
539 light-energy dissipation in ryegrass (Lolium perenne) when source/sink ratios become high at
540 a naturally grazed Free Air CO2 Enrichment (FACE) site. *Functional Plant Biology* **33**, 1045-
541 1053.
542
543 Hernandez-Clemente R, Navarro-Cerrillo RM, Suarez L, Morales F, Zarco-Tejada PJ (2011)
544 Assessing structural effects on PRI for stress detection in conifer forests. *Remote Sensing of*
545 *Environment* **115**, 2360-2375.
546
547 Hilker T, Coops NC, Hall FG, Black TA, Wulder MA, Nesic Z, Krishnan P (2008a)
548 Separating physiologically and directionally induced changes in PRI using BRDF models.
549 *Remote Sensing of Environment* **112**, 2777-2788.
550
551 Hilker T, Coops NC, Schwalm CR, Jassal RS, Black TA, Krishnan P (2008b) Effects of
552 mutual shading of tree crowns on prediction of photosynthetic light-use efficiency in a coastal
553 Douglas-fir forest. *Tree Physiology* **28**, 825-834.

554
555 Hilker T, Hall FG*, et al.* (2010) Remote sensing of photosynthetic light-use efficiency across
556 two forested biomes: Spatial scaling. *Remote Sensing of Environment* **114**, 2863-2874.
557
558 Hilker T, Nesic Z, Coops NC, Lessard D (2009) A New, Automated, Multiangular
559 Radiometer Instrument · for Tower-Based Observations of Canopy Reflectance (AMSPEC
560 II). *Instrumentation Science & Technology* **38**, 319-340.
561
562 Kalina J, Slovák V (2004) The inexpensive tool for the determination of projected leaf area.
563 *Ekologia-Bratislava* **23**, 163-167.
564
565 Kokaly RF, Clark RN (1999) Spectroscopic determination of leaf biochemistry using band-
566 depth analysis of absorption features and stepwise multiple linear regression. *Remote Sensing*
567 *of Environment* **67**, 267-287.
568
569 Kurasová I, Čajánek M, Kalina J, Urban O, Špunda V (2002) Characterization of acclimation
570 of Hordeum vulgare to high irradiation based on different responses of photosynthetic activity
571 and pigment composition. *Photosynthesis Research* **72**, 71-83.
572
573 Kurasová I, Kalina J, Urban O, Štroch M, Špunda V (2003) Acclimation of two distinct plant
574 species, spring barley and Norway spruce, to combined effect of various irradiance and CO2
575 concentration during cultivation in controlled environment. *Photosynthetica* **41**, 513-523.
576
577 Lichtenthaler HK (1987) Chlorophylls and carotenoids: Pigments of photosynthetic
578 biomembranes. *Methods in Enzymology* **148**, 350-382.
579
580 Lichtenthaler HK, Ac A, Marek MV, Kalina J, Urban O (2007) Differences in pigment
581 composition, photosynthetic rates and chlorophyll fluorescence images of sun and shade
582 leaves of four tree species. *Plant Physiology and Biochemistry* **45**, 577-588.
583
584 Malenovský Z, Albrechtová J, Lhotáková Z, Zurita-Milla R, Clevers J, Schaepman ME,
585 Cudlín P (2006a) Applicability of the PROSPECT model for Norway spruce needles.
586 *International Journal of Remote Sensing* **27**, 5315-5340.

587

588 Malenovský Z, Ufer CM, Lhotáková Z, Clevers JGPW, Schaepman ME, Albrechtová J,
589 Cudlín P (2006b) A new hyperspectral index for chlorophyll estimation of a forest canopy:
590 Area under curve Normalized to Maximal Band depth between 650-725 nm. *EARSeL*
591 *eProceedings* **5**, 161-172.

592

593 Mesarch MA, Walter-Shea EA, Asner GP, Middleton EM, Chan SS (1999) A revised
594 measurement methodology for conifer needles spectral optical properties: Evaluating the
595 influence of gaps between elements. *Remote Sensing of Environment* **68**, 177-192.

596

597 Moran JA, Mitchell AK, Goodmanson G, Stockburger KA (2000) Differentiation among
598 effects of nitrogen fertilization treatments on conifer seedlings by foliar reflectance: a
599 comparison of methods. *Tree Physiology* **20**, 1113-1120.

600

601 Myneni RB, Williams DL (1994) On the Relationship between FAPAR and NDVI *Remote*
602 *Sensing of Environment* **49**, 200-211.

603

604 Nakaji T, Oguma H, Fujinuma Y (2006) Seasonal changes in the relationship between
605 photochemical reflectance index and photosynthetic light use efficiency of Japanese larch
606 needles. *International Journal of Remote Sensing* **27**, 493-509.

607

608 Nichol CJ, Lloyd J, Shibistova O, Arneth A, Roser C, Knohl A, Matsubara S, Grace J (2002)
609 Remote sensing of photosynthetic-light-use efficiency of a Siberian boreal forest. *Tellus*
610 *Series B-Chemical and Physical Meteorology* **54**, 677-687.

611

612 Nichol CJ, Rascher U, Matsubara S, Osmond B (2006) Assessing photosynthetic efficiency in
613 an experimental mangrove canopy using remote sensing and chlorophyll fluorescence. *Trees-*
614 *Structure and Function* **20**, 9-15.

615

616 Peñuelas J, Filella I, Gamon JA (1995) Assessment of photosynthetic radiation-use efficiency
617 with spectral reflectance. *New Phytologist* **131**, 291-296.

618

R Development Core Team (2010) R: A language and environment for statistical computing. R Foundation for Statistical Computing. *Vienna, Austria.* **ISBN 3-900051-07-0**.

Ripullone F, Rivelli AR, Baraldi R, Guarini R, Guerrieri R, Magnani F, Penuelas J, Raddi S, Borghetti M (2011) Effectiveness of the photochemical reflectance index to track photosynthetic activity over a range of forest tree species and plant water statuses. *Functional Plant Biology* **38**, 177-186.

Sarijeva G, Knapp M, Lichtenthater HK (2007) Differences in photosynthetic activity, chlorophyll and carotenoid levels, and in chlorophyll fluorescence parameters in green sun and shade leaves of Ginkgo and Fagus. *Journal of Plant Physiology* **164**, 950-955.

Sims DA, Gamon JA (2002) Relationships between leaf pigment content and spectral reflectance across a wide range of species, leaf structures and developmental stages. *Remote Sensing of Environment* **81**, 337-354.

Stylinski CD, Gamon JA, Oechel WC (2002) Seasonal patterns of reflectance indices, carotenoid pigments and photosynthesis of evergreen chaparral species. *Oecologia* **131**, 366-374.

Suarez L, Zarco-Tejada PJ, Sepulcre-Canto G, Perez-Priego O, Miller JR, Jimenez-Munoz JC, Sobrino J (2008) Assessing canopy PRI for water stress detection with diurnal airborne imagery. *Remote Sensing of Environment* **112**, 560-575.

Štroch M, Kuldová K, Kalina J, Špunda V (2008) Dynamics of the xanthophyll cycle and non-radiative dissipation of absorbed light energy during exposure of Norway spruce to high irradiance. *Journal of Plant Physiology* **165**, 612-622.

Štroch M, Vrábl D, Podolinská J, Kalina J, Urban O, Špunda V (2010) Acclimation of Norway spruce photosynthetic apparatus to the combined effect of high irradiance and temperature. *Journal of Plant Physiology* **167**, 597-605.

651 Thayer SS, Björkman O (1992) Carotenoid distribution and deepoxidation in thylakoid
652 pigment- protein complexes from cotton leaves and bundle-sheath cells of maize.
653 *Photosynthesis Research* **33**, 213-225.
654
655 Tucker CJ (1979) Red and photographic infrared linear combinations for monitoring
656 vegetation *Remote Sensing of Environment* **8**, 127-150.
657
658 Ustin SL, Asner GP, Gamon JA, Huemmrich KF, Jacquemoud S, Schaepman M, Zarco-
659 Tejada P, Ieee (2006) Retrieval of Quantitative and Qualitative Information about Plant
660 Pigment Systems from High Resolution Spectroscopy. In '2006 Ieee International Geoscience
661 and Remote Sensing Symposium, Vols 1-8' pp. 1996-1999. (Ieee: New York)
662
663 van Amerongen H, van Grondelle R (2001) Understanding the energy transfer function of
664 LHCII, the major light-harvesting complex of green plants. *Journal of Physical Chemistry B*
665 **105**, 604-617.
666
667 Way DA, Sage RF (2008) Elevated growth temperatures reduce the carbon gain of black
668 spruce [Picea mariana (Mill.) BSP]. *Global Change Biology* **14**, 624-636.
669
670
671
672
673
674
675
676
677
678
679
680
681
682
683

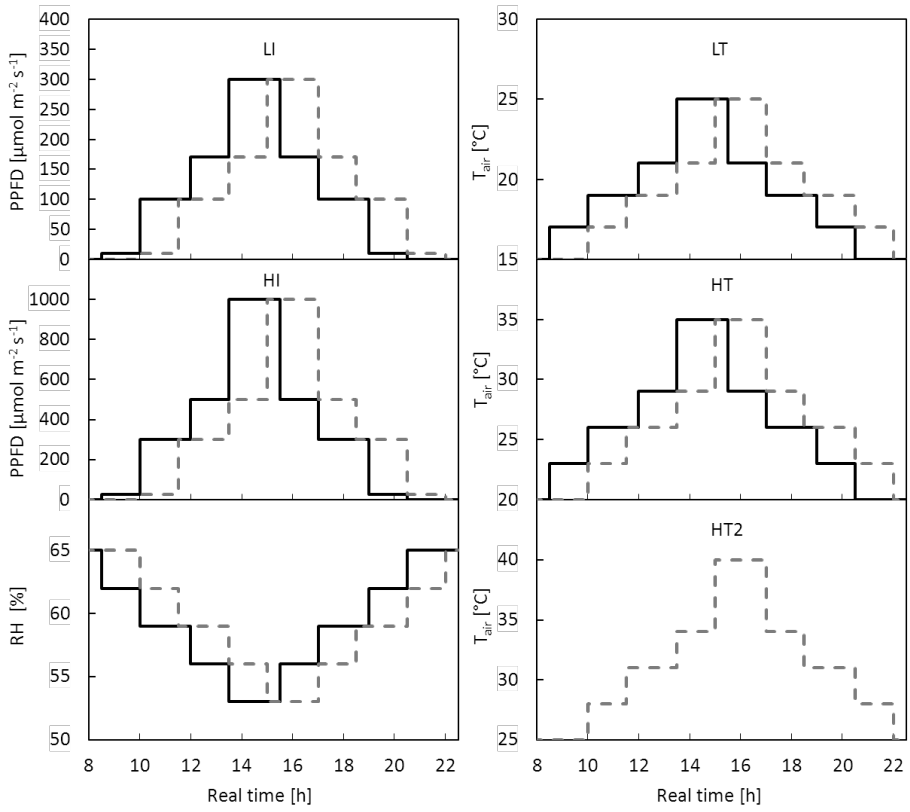

Fig. 1: Diurnal courses of microclimatic conditions in both growth chambers. Photosynthetic photon flux density (PPFD) and air temperature (T_{air}) were combined in LI-LT, HI-LT, HI-HT and HI-HT2 treatments. The daily course of relative air humidity (RH_{air}) remained stable (50-65%) throughout the whole experiment. A black solid line indicates the real time schedule of the regime in chamber one, whereas a grey dashed line indicates the regime in chamber two.

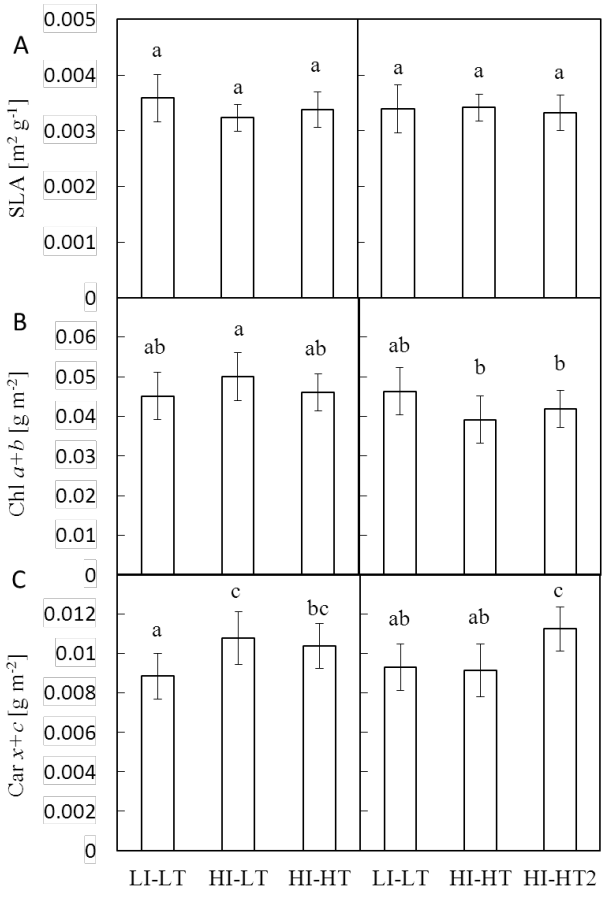

Fig. 2: (A) Specific leaf area (SLA), (B) total content of chlorophylls (Chl *a*+*b*) and (C) the content of carotenoids (Car *x*+*c*) measured at the end of the nighttime period (i.e. after 12 h of darkness) for needles acclimated to four irradiation-temperature regimes (LI-LT, HI-LT, HI-HT, HI-HT2). The left-hand side column represents measurements in growth chamber one, the right-hand side column in chamber two. Means (columns) and standard deviations (bars) are presented (n=5). Data followed by the same letter indicate statistically insignificant differences ($P < 0.05$; Student's t-test).

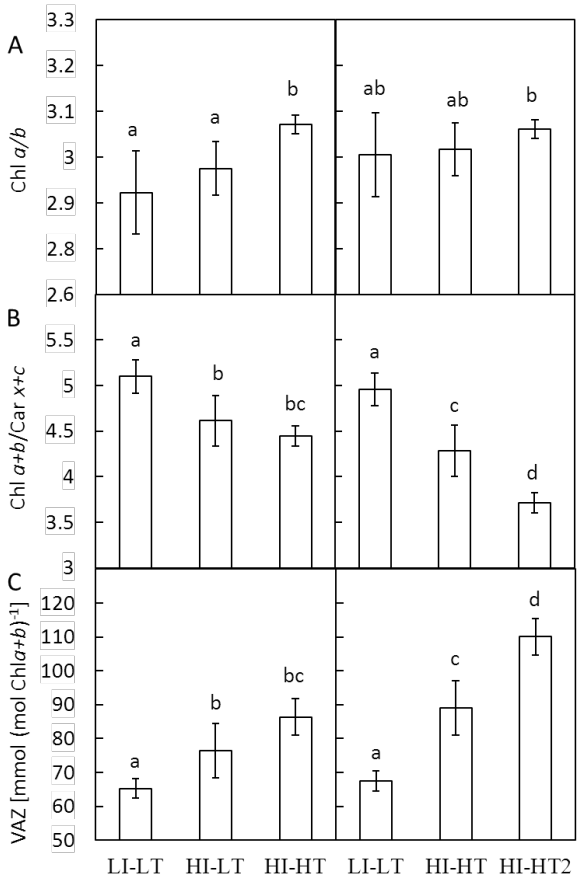

Fig. 3: (A) Ratio of chlorophyll *a* to chlorophyll *b* (Chl *a/b*), (B) ratio of total chlorophylls to total carotenoids (Chl *a*+*b*/Car *x*+*c*) and (C) the content of xanthophyll cycle pigments per total chlorophyll content (VAZ/Chl *a*+*b*) estimated for the particular acclimation regimes. Needles were sampled at the end of the nighttime period on the last day of acclimation to the given regime. The left-hand side column shows measurements of chamber one, the right-hand side column measurements of chamber two. Means (columns) and standard deviations (bars) are presented (n=5). Data followed by the same letter indicate statistically insignificant differences ($P < 0.05$; Student's t-test).

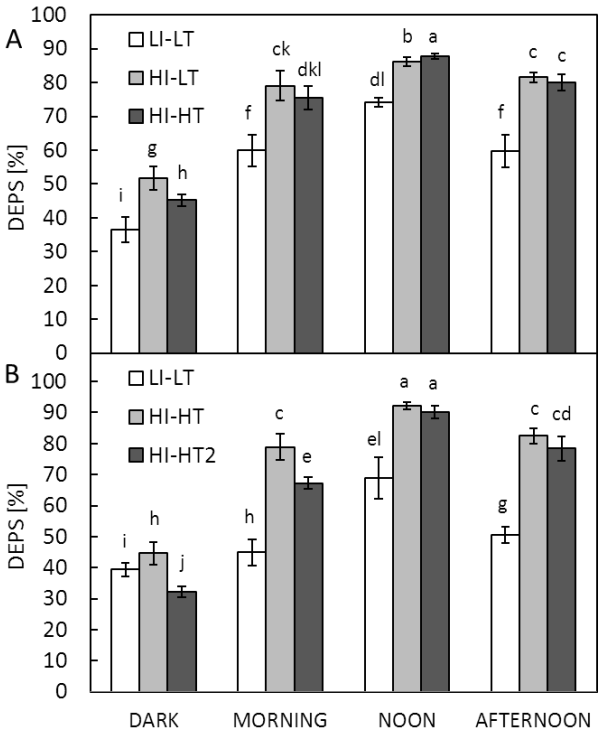

Fig. 4: The de-epoxidation state of the xanthophyll cycle pigments [DEPS = (Z+A)/(V+A+Z)*100] determined in the daily course at the end of the particular acclimation regimes. (A) data of chamber one, (B) data of chamber two. Means (columns) and standard deviations (bars) are presented (n=5) for needle samples examined per treatment and time of the day. Data followed by the same letter indicate statistically insignificant differences ($P < 0.05$; Student's t-test).

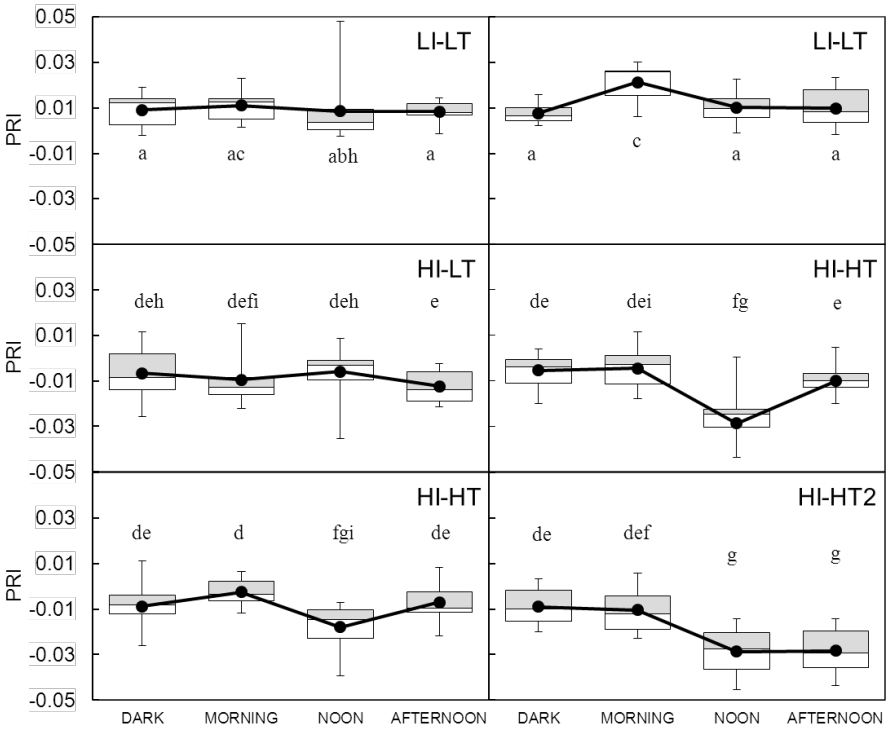

Fig. 5: Daily courses of the Photochemical Reflectance Index (PRI) computed from the database of 205 measured reflectance spectra. Needles were sampled during a last simulated daytime period of acclimation to the given regime (LI-LT, HI-LT, HI-HT, and HI-HT2). The left-hand side column presents daily courses of PRI for measurements in chamber one, the right-hand side column shows PRI measurements in chamber two. Central lines represent the medians, boxes represent 50% of the data, and whiskers represent the minimum and maximum values. Dark dots connected with the straight line represent an average of 7-10 values measured during each cycle. Data followed by the same letter indicate statistically insignificant differences ($P < 0.05$; Mann–Whitney U-test).

Pozn: v textu se odvolavame na rozdíly významné, ale někde jsou hodnoty takové, že významný rozdíl neukazují, např komora 1 LT-LT poledne vs komota 1 HI-LT tma – je tam jedna až pár hodnot, které by mohly výstup zpochybnit, ale pro vice jak 90 procent údajů to neplatí

-> pokud je potreba udelej zmenu v textu taka by to odpovidalo grafu!!!

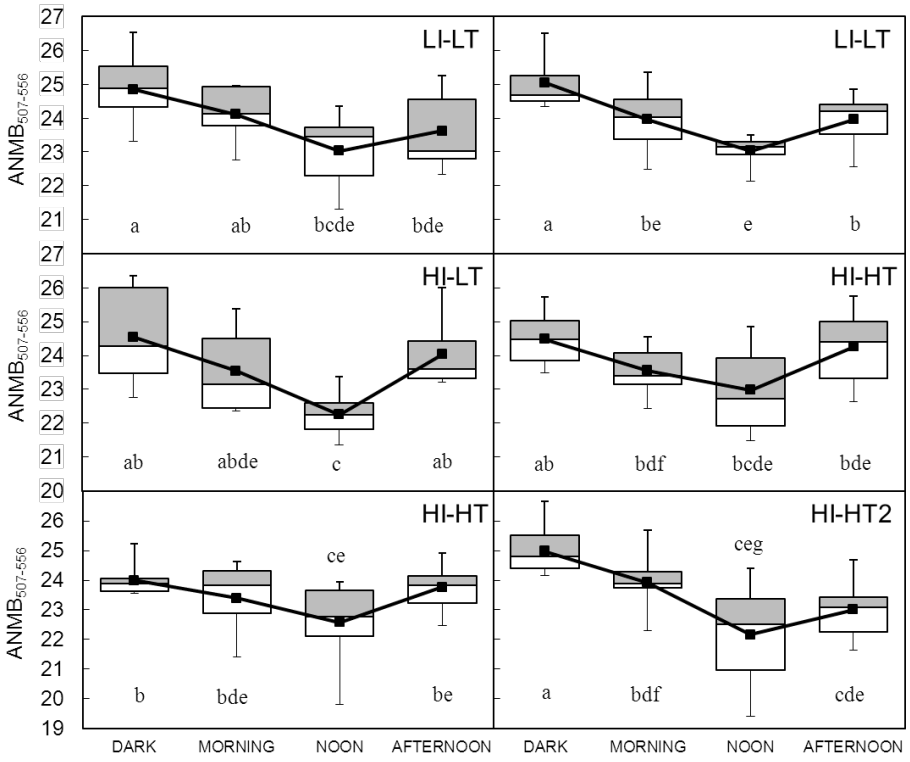

Fig. 6: Daily course of $ANMB_{507-556}$ computed from the database of 205 measured reflectance spectra. Needles were sampled during the last simulated daytime period of acclimation to the given regime (LI-LT, HI-LT, HI-HT, and HI-HT2). The left-hand side column presents daily courses of $ANMB_{507-556}$ for measurements in chamber one, the right-hand side column shows measurements in chamber two. Central lines represent the medians, boxes represent 50% of the data, and whiskers represent the minimum and maximum values. Dark dots connected with the straight line represent an average of 7-10 values measured during each cycle. Data followed by the same letter indicate statistically insignificant differences ($P < 0.05$; Mann–Whitney U-test).

Pozn: nicneříkající statistika, není zdůvodněno v textu proč byla počítána, co říká

-> zminil jsem v textu srovnavaci test, predpokladam ze vsechny P pro Mann–Whitney U-test jsou < 0.05 ne > ???!!! … potreba prekontrolovat v celem textu i pro T-test!!!

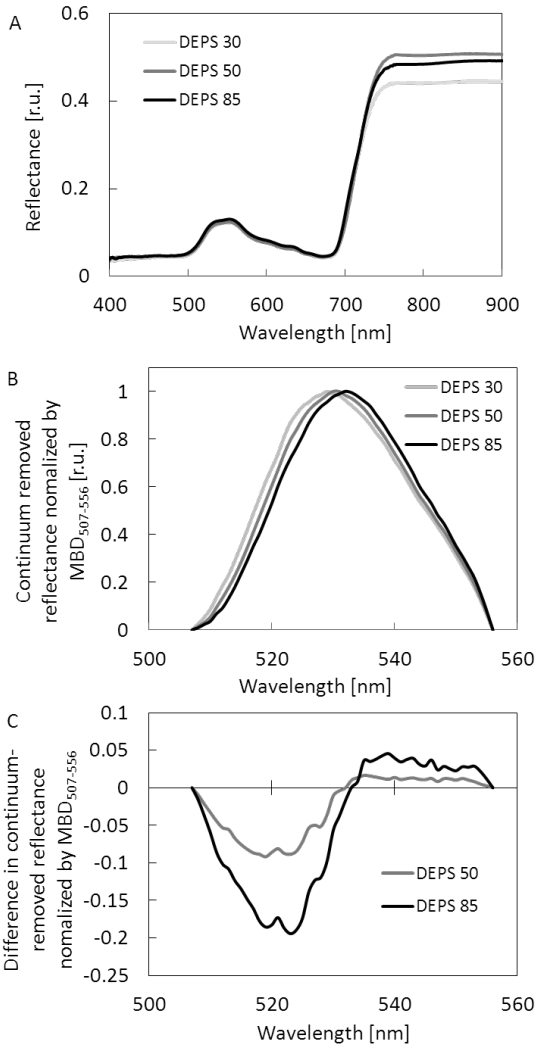

Fig 7. A) Reflectance signatures measured for needle samples of the same gap fraction size (0.51) at three DEPS levels (30, 50 and 85%), B) continuum-removed reflectance normalized to the maximum band depth (MBD) between 507 and 556 nm for the same reflectance signatures, C) MBD normalized continuum-removed reflectance of needle samples with DEPS equal to 50% and 85% substracted from the same reflectance transformation of a sample with DEPS equal to 30% (calculated from the curves of Fig. 7B).

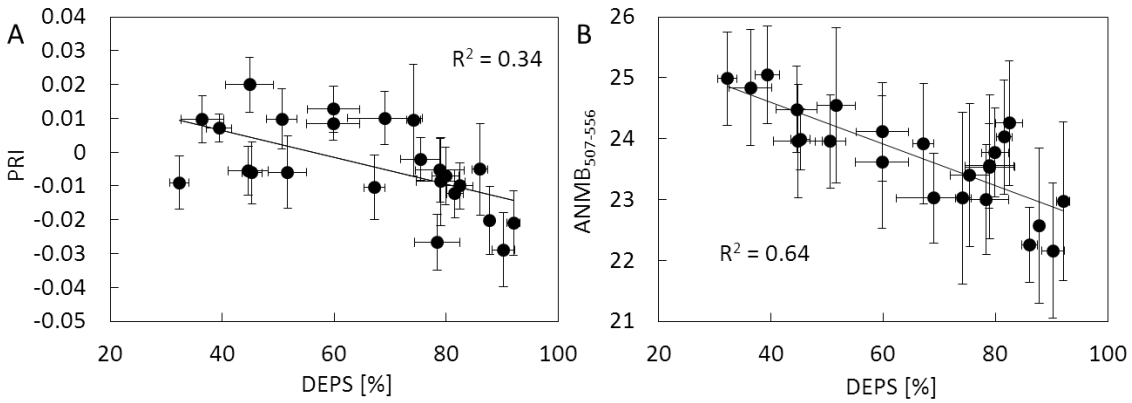

Fig. 8: Dependency between (A) mean values of PRI and DEPS (n = 24), and (B) mean values of $ANMB_{507-556}$ and DEPS (n = 24). Average values and standard deviation of both vegetation indices and DEPS are calculated from 5-10 measurements acquired during daily courses of each treatment.

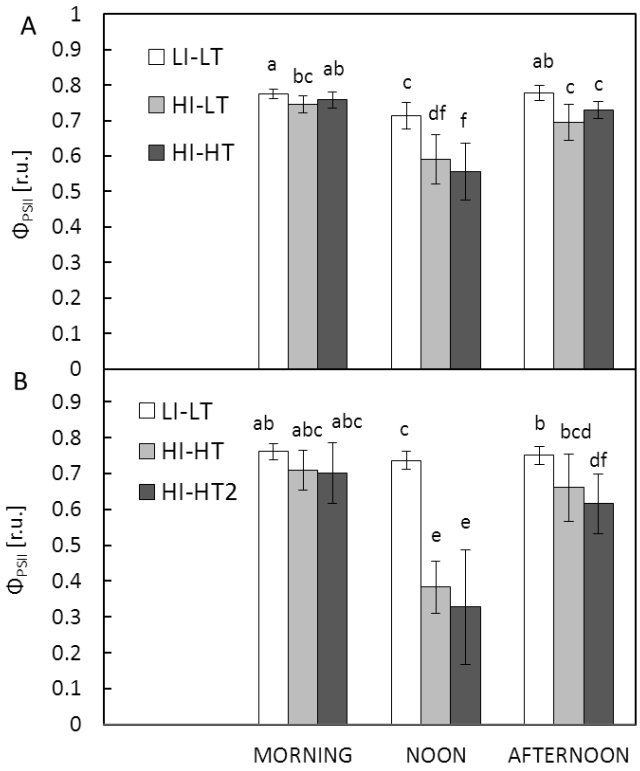

Fig. 9: Daily changes in quantum yield of photosystem II photochemistry (Φ_{PSII}) for plants acclimated to the particular LI-LT, HI-LT, HI-HT and HI-HT2 regime. (A) measurements of chamber one, (B) measurements of chamber two. Values are means ± SD for 5 needle samples examined per acclimation regime at the given time of the day. Data followed by the same letter indicate statistically insignificant differences ($P < 0.05$; Student's t-test).

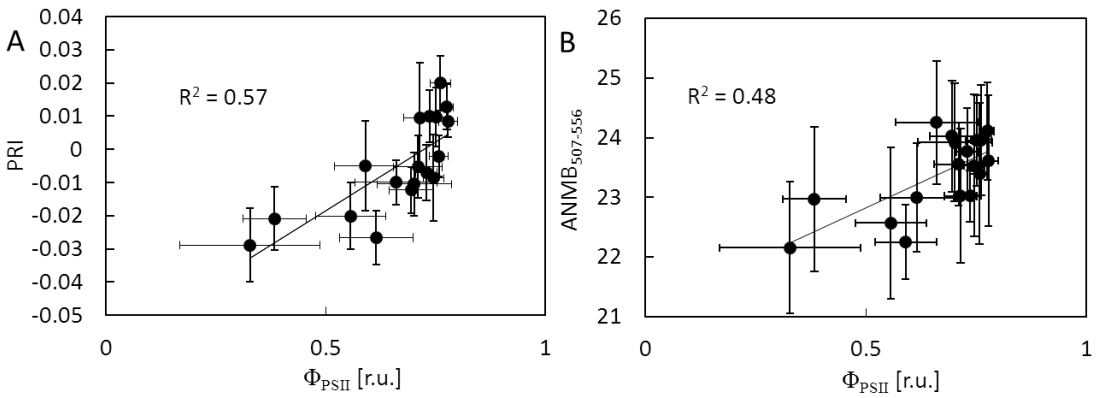

Fig. 10: Linear regression between quantum yield of photosystem II photochemistry (Φ_{PSII}) and A) PRI, and B) $ANMB_{507-556}$ calculated from directional-hemispherical reflectance of spruce needles acclimated to the LI-LT, HI-LT, HI-HT and HI-HT2 regimes (n=18). Average values and standard deviation of both vegetation indices and Φ_{PSII} are calculated from 5-10 measurements acquired for each treatment.